

TiO₂-supported metal oxide catalysts for low-temperature selective catalytic reduction of NO with NH₃

I. Evaluation and characterization of first row transition metals

Donovan A. Peña, Balu S. Uphade,¹ and Panagiotis G. Smirniotis*

Chemical and Materials Engineering Department, University of Cincinnati, Cincinnati, OH 45221-0012, USA

Received 29 April 2003; revised 28 July 2003; accepted 3 September 2003

Abstract

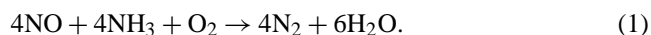
Low-temperature SCR of NO with NH₃ in the presence of excess oxygen on the oxides of V, Cr, Mn, Fe, Co, Ni, and Cu supported on anatase TiO₂ has been studied. Among the catalysts tested, Mn/TiO₂ supported on Hombikat TiO₂ provided the best performance with 100% N₂ selectivity and complete NO conversion at temperatures as low as 393 K under numerous conditions. The catalytic performance for various transition metal oxides supported on TiO₂ decreased in the following order: Mn > Cu ≥ Cr ≫ Co > Fe ≫ V ≫ Ni. For Mn-based catalysts the activity increases with an increase in Mn loading and the reaction temperature. TiO₂ alone did not give any NO conversion at ≤ 573 K, and calcination at low temperature (≤ 673 K) is preferable. XRD coupled with XPS confirmed the presence of MnO₂ as a major phase (peak at 642.2 eV) with Mn₂O₃, and partially undecomposed Mn-nitrate as the minor phases for supported manganese catalysts. It is proposed that MnO₂ contributes to the high activity of Mn/TiO₂. XPS results also confirmed a higher concentration of active metal oxides on the surface of Mn/TiO₂ compared to the other catalysts. The NH₃ FT-IR study showed the presence of Lewis acid sites for the most active catalysts, while the peak corresponding to Brønsted acid sites was weak or absent. This strongly suggests that Brønsted acid sites are not necessary for the reaction to occur at low temperatures. The H₂ TPR study indicated the difficulty of reducing Mn oxide when the metal loading is low and/or the catalysts are calcined at temperatures higher than 773 K. It is concluded that lower catalyst calcination temperatures, Lewis acidity, the redox properties of metal oxides and their higher surface concentration are important for very high SCR activity at low temperatures. Mn/TiO₂ provided the best performance at 50,000 h⁻¹ when the catalysts were tested in the presence of 11 vol% H₂O. Under these conditions, the catalytic activity of the transition metal oxides decreases in the following order: Mn > V ≫ Co > Cu > Cr > Fe ≫ Ni. © 2003 Elsevier Inc. All rights reserved.

Keywords: Low-temperature SCR; Ammonia; Nitric oxide reduction; Titania; Transition metal oxides

1. Introduction

Nitrogen oxides (NO_x) emitted from automobiles and stationary sources such as oil- and coal-fired power plants, waste incinerators, industrial ovens, and chemical processes (i.e., nitric acid production plants) are major causes for acid rain, smog, and ozone depletion [1–3]. Selective catalytic reduction (SCR) of NO_x to N₂ using NH₃ as a reductant is now considered to be the most effective process for the treatment of stack gases from stationary sources. The general reaction

occurring is



The well-known industrial catalyst for this process is based on V₂O₅/TiO₂ (anatase) promoted with either WO₃ or MoO₃ [4–9]. The required operating temperature for the above industrial catalyst is typically 573–673 K. This makes it necessary to locate the SCR unit upstream of the desulfurizer and/or particulate control device in order to avoid reheating the flue gas. Despite the low sensitivity of this catalyst to SO₂ poisoning, deactivation does occur. The life of the catalyst is shortened because of high concentrations of SO₂ and ash in the flue gas. This can be avoided by locating the SCR reactor downstream in the tail-end configuration, where the flue gas is relatively clean after passing through

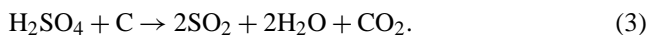
* Corresponding author.

E-mail address: Panagiotis.Smirniotis@UC.EDU (P.G. Smirniotis).

¹ Current address: Chemical Engineering Division, National Chemical Laboratory, Pune 411 008, India.

the desulfurizer and particulate removal device. This strategy would be especially advantageous for high-sulfur coals, as the removal of SO₂ before NO_x removal would minimize both the catalyst deactivation and the detrimental oxidation of SO₂ to SO₃. However, the flue gas temperature at this location drops below 433 K, which makes it necessary to reheat the flue gas back to the SCR operating temperature. This makes the overall operation very expensive. One solution to this problem is the development of an inexpensive low-temperature SCR system that operates at ≤ 423 K. This would eliminate the need to reheat the stack gas and increase the operational lifetime of the catalyst relative to existing configurations, which results in a lower investment and also a thermally more efficient process.

Supported transition metal oxides, such as MnO_x/Al₂O₃ [10–12], CuO/Al₂O₃ [13], CuO/TiO₂ [14], Fe₂O₃/TiO₂ [15], and V₂O₅/activated carbon [16–18], are shown to be active in medium temperature SCR of NO with NH₃ in the presence of excess oxygen. Recent efforts have been made to develop robust catalysts for low-temperature SCR of NO using NH₃ [19,20]. Industrial researchers have particularly shown an interest in this area. Taking into account the various advantages of low-temperature operation, a process based on carbon as a catalyst has been developed (Bergbau-Farschuang and Mitsui) for simultaneous removal of H₂S, SO₂, and NO_x from industrial process gases and off gases. The reaction products of H₂S and SO₂ are adsorbed on the carbon catalyst whereas NO_x is reduced by NH₃ according to reaction (1) at ≥ 363 K. However, carbon has the danger of getting consumed slowly [reaction (3)], thereby decreasing steadily the activity and available capacity of carbon during operation [21].



Shell [22] and Rhône-Poulenc [23] also have developed V-based supported catalysts that are claimed to operate in the temperature range of 313–523 K. The good low-temperature performance of Shell's industrial processes is attributed to a better reactor design (lateral flow) and an improved catalyst preparation method using promoters such as Fe, Mo, and Co.

This paper describes work performed in our laboratory [24,25] in an effort to find active catalysts for the SCR of NO at low temperatures (≤ 423 K). Catalysts were prepared from various transition metal oxides (V, Cr, Mn, Fe, Co, Ni, and Cu) deposited by the solution impregnation method using nitrate or acetate precursors on titania. It is shown here that MnO_x/TiO₂ catalysts can operate effectively below 423 K with both high NO conversion and N₂ selectivity. In Part II of this work, in situ FT-IR studies have been used extensively to develop a low-temperature SCR reaction mechanism.

2. Experimental

2.1. Catalyst preparation

The TiO₂ used in this study was Hombikat UV 100 from Sachtleben Chemie. As determined by N₂ adsorption, it had a specific surface area of 309 m²/g, a pore volume of 0.37 cm³/g, and a pore diameter of 4.5 nm. The transition metal oxides were deposited using aqueous solutions of their nitrates by the solution impregnation method as previously reported [25,26]. In one of the catalyst preparation experiments, manganese acetate was also used as the precursor for comparison. In a typical synthesis, 50 ml of deionized water was added to a 100-ml beaker containing 1.0 g of support. The mixture was heated to 343 K under continuous stirring. A measured quantity of nitrate or acetate precursor was then added, and the mixture was evaporated to dryness. The paste obtained was further dried overnight at 383 K, ground, and sieved (80–120 mesh). The calcination of the catalysts was performed at 673 K for 2 h in a flow of O₂ (4.0% in helium).

2.2. Characterization of supports and catalysts

Prior to characterization, the samples were calcined at 673 K for 2 h in O₂ (4.18% in He) at a total flow rate of 20 ml/min. The catalysts were stored in a vacuum oven maintained at 328 K and 30 inches Hg of vacuum.

X-ray diffraction was used to identify the anatase and rutile phases of titania and the crystalline phases of any transition metal oxides deposited on titania. XRD studies were performed on a Siemens D500 diffractometer with a Cu-K_α radiation source (wavelength 1.5406 Å). Aluminum holders were used to support the samples in XRD measurements. Anatase and rutile phases of titania were determined from the strongest peaks corresponding to anatase [2θ = 25.3° for the (101) reflection of anatase] and rutile [2θ = 27.5° for the (110) reflection of rutile]. A combination of Raman and XRD results was used to determine the crystalline phases of titania. Self-supported pellets (100–150 mg) were used for the Raman study, which was collected using an Ar laser at 2 mW under ambient conditions.

The specific surface areas were measured by nitrogen adsorption at 77 K by the BET method using a Micromeritics Gemini 2360. Pore-size measurements were performed using a Micromeritics ASAP 2010. Catalysts were pretreated in situ at 523 K under vacuum, and the analysis of the supports was done at 77 K under vacuum.

X-ray photoelectron spectroscopy (XPS) was used to analyze the atomic surface concentration on each catalyst. The spectra were recorded on a Perkin-Elmer Model 5300 X-ray photoelectron spectrometer using Mg-K_α (1253.6 eV) as a radiation source at 300 W. The spectra were recorded in the fixed analyzer transmission mode with pass energies of 89.45 and 35.75 eV for recording survey and high-resolution spectra, respectively. The powdered catalysts were mounted

onto the sample holder and degassed overnight at room temperature at a pressure on the order of 10^{-7} Torr. Binding energies (BE) were measured for C 1s, O 1s, Ti 2p, V 2p, Mn 2p, Cr 2p, Ni 2p, and Cu 2p. Since the tape used to mount the sample was a source of carbon contamination, the surface composition of carbon is not included in the tables. Recorded Auger spectra for Mn, Cr, and Ni were very weak. Sample charging effects were eliminated by correcting the observed spectra with the Ti 2p_{3/2} binding energy value of 458.5 eV. An estimated error of 0.1 eV can be considered for all the measurements. The spectra were smoothed, and a nonlinear background was subtracted. Peaks were deconvoluted, and the fitting was performed using a convolution of Gaussian and Lorentzian curves. Quantification was accomplished by determining the elemental peak areas following a Shirley background subtraction. Quantitative analysis was carried out using the sensitive factors supplied with the instrument.

FT-IR and NH₃-TPD were used to characterize and quantify the acidity of the catalysts, respectively. The FT-IR experiments were performed with a Bio-Rad spectrophotometer (FTS-040). Circular self-supporting thin wafers (8 mm diameter) prepared using 6–8 mg catalyst were used for the study. The wafers were placed in a high-temperature cell with AgBr windows and purged with prepurified grade helium (30 ml/min) at 673 K for 2 h to remove any impurities before cooling down to 323 K. NH₃ (4.4 vol% in He) was introduced to the cell and continued flowing (30 ml/min) for a total of 1 h at 323 K to ensure complete saturation of the sample. Helium (30 ml/min) was then replaced by NH₃ and the temperature was increased to 373 K. Physisorbed ammonia was removed by flushing the wafer with He for at least 4 h. Subsequently, the FT-IR spectra were recorded by desorbing NH₃ at 373 K. All the spectra were recorded at 373 K and normalized to avoid inconsistencies in the results.

TPD of NH₃ was used to measure the total acidity of the catalysts. The experiments were performed on a custom-made TCD setup using 50 mg of catalyst. Prior to the experiments the catalysts were pretreated at 773 K for 1 h in a highly pure He (30 ml/min) stream. The furnace temperature was lowered to 373 K, and the samples were then treated with anhydrous NH₃ (4.05% in He) at a flow rate of 30 ml/min for 1 h. Physisorbed NH₃ was removed by flushing the catalyst with He at 373 K for 3–5 h before starting the TPD experiments. Experimental runs were recorded by heating the sample in He (30 ml/min) from 373 to 773 K at a heating rate of 5 K/min and finally keeping the temperature constant for 1 h at 773 K to ensure complete ammonia desorption.

The H₂-TPR experiments were performed on a custom-made setup using 100 mg of calcined catalyst. The catalysts were pretreated at 673 K for 1 h in a highly pure He (25 ml/min) stream. The furnace temperature was lowered to 373 K, and then the feed containing 6.0 vol% H₂ in He was fed at a flow rate of 25 ml/min. H₂-TPR runs were performed by heating the sample from 373 to 1173 K at a linear

heating rate of 5 K/min and finally keeping the temperature constant for 1 h at 1173 K to ensure complete metal oxide reduction. The hydrogen consumed in the TPR was measured by a TCD.

2.3. Catalytic experiments

The SCR of NO at atmospheric pressure was carried out in a fixed-bed quartz reactor (i.d. 6 mm) containing calcined catalyst (80–120 mesh). Oxygen (Wright Bros., 4.18% in He), ammonia (Matheson, 3.89% in He), and nitric oxide (Air Products, 2.0% in He) were used as received. The reaction temperature was measured by a type K thermocouple inserted directly into the catalyst bed. Experiments were performed under two different reaction conditions. While the concentration of O₂ remained constant (2 vol%), the reactant concentrations and GHSVs varied between the two cases. In the first case at 8000 h⁻¹, the inlet concentrations of NO and NH₃ were each 2000 ppm. The reactants and products were analyzed on-line using a Quadrupole mass spectrometer (MKS PPT-RGA). In the second case at 50,000 h⁻¹, the inlet concentrations of NO and NH₃ were each set at 400 ppm. The reactants and products were analyzed using a GC (GOW-MAC) with Porapak Q and Carboxen 1000 columns and a NO_x analyzer (Eco Physics CLD 70S). The definitions used for NO conversion and nitrogen selectivity are as follows:

$$\text{NO conversion} = 100 \times (\text{NO}_{\text{in}} - \text{NO}_{\text{out}}) / \text{NO}_{\text{in}}, \quad (4)$$

$$\text{N}_2 \text{ selectivity} = 100 \times \{ \text{N}_2 / (\text{N}_2 + \text{N}_2\text{O}) \}. \quad (5)$$

3. Results and discussion

3.1. Surface area and pore-size distribution

The BET surface area values of the various metal oxides deposited on TiO₂ are compared in Table 1. The results show the expected drop in surface area upon impregnation of the transition metal oxides on TiO₂. The drop was most severe when vanadia was deposited. It is reported in the literature that V₂O₅/TiO₂ (anatase) is quite unstable and that vanadia facilitates transformation of the metastable anatase phase of titania into the thermodynamically more stable rutile phase at any temperature and pressure [27]. Vanadia also favors the sintering of anatase along with the corresponding decrease in surface area [28]. Therefore, to retard the phase transition and the loss of surface area, WO₃ or MoO₃ is added to commercial V₂O₅/TiO₂ (anatase) catalysts. The drop in surface area was not very severe when metal oxides of Mn, Cr, and Cu were deposited. This suggests that impregnation with Mn, Cr, and Cu probably inhibits the sintering and/or phase transformation of the support and also enhances dispersion of transition metal oxides on the supports. In fact, the effect of Mn loading on TiO₂ suggests that overall surface area improves with an increase in metal loading on the

Table 1
Properties of catalysts used in the present study

Catalyst ^a	Loading (wt%)	SSA (m ² /g)	XRD phases observed	Total acidity (μmol/g)
TiO ₂	n/a	309	Anatase	n.d.
V ^b	20	51	None	9.8
Cr ^c	20	143	Cr ₂ O ₃	55.8
Mn ^c	5	n.d.	n.d.	n.d.
Mn ^c	10	n.d.	n.d.	n.d.
Mn ^c	12.5	173	n.d.	n.d.
Mn ^d	12.5	165	n.d.	n.d.
Mn ^c	15	n.d.	n.d.	n.d.
Mn ^c	20	204	Mn ₂ O ₃	23.2
Mn ^c	25	n.d.	n.d.	n.d.
Fe ^c	20	169	Fe ₂ O ₃	33.6
Co ^c	20	160	Co ₃ O ₄	31.6
Ni ^c	20	163	NiO	42.7
Cu ^c	20	140	CuO	12.5

n.d., not determined; n/a, not applicable.

^a Calcined at 400 °C for 2 h in O₂ + He flow.

^b Ammonium metavanadate + oxalic acid.

^c Nitrate precursor.

^d Acetate precursor.

support. In conclusion, the results in Table 1 clearly indicate that with the exception of V₂O₅/TiO₂ catalyst, the surface area of other transition metals supported on TiO₂ catalysts is higher.

3.2. X-ray diffraction and Raman spectroscopy

3.2.1. TiO₂

The phase compositions of titania determined from XRD and Raman spectroscopy results are described below. Only anatase is observed from the XRD results. As reported in the literature [29], five peaks from Raman spectroscopy near 638, 515, 396, 196, and 144 cm⁻¹ that correspond to anatase were observed (not shown). The broadening of the peak at 144 cm⁻¹ in Hombikat TiO₂ also indicates the possible presence of the brookite phase of TiO₂, as its two most intense peaks (127 and 150 cm⁻¹) should be in the vicinity of 144 cm⁻¹.

3.2.2. Transition metal oxides

The XRD patterns of the catalysts calcined at 673 K for 2 h are shown in Fig. 1, and the observed crystalline XRD phases for these catalysts are also tabulated in Table 1. None of the XRD spectra presented here give intense or sharp peaks for transition metal oxides despite having relatively high metal concentrations (20.0 wt%) on the titania support. This may be due to the high dispersion and/or low crystalline nature (amorphous) of the metal oxides on the support. MnO₂ at 2θ values of 28.9, 37.7, and 57.1° with relative intensities of 100, 55, and 55%, respectively (JCPDS File No. 24-0735), was observed as the only phase for supported manganese oxide catalysts. The crystalline phase of Mn₂O₃ (Fig. 1) could not be observed; however, it will be shown below that at least two different oxidation states could

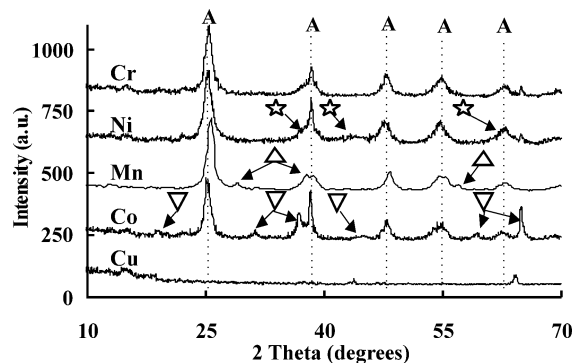


Fig. 1. XRD spectra of 20 wt% transition metals supported on Hombikat TiO₂ (A, anatase; ☆, NiO; Δ, MnO₂; ∇, Co₃O₄).

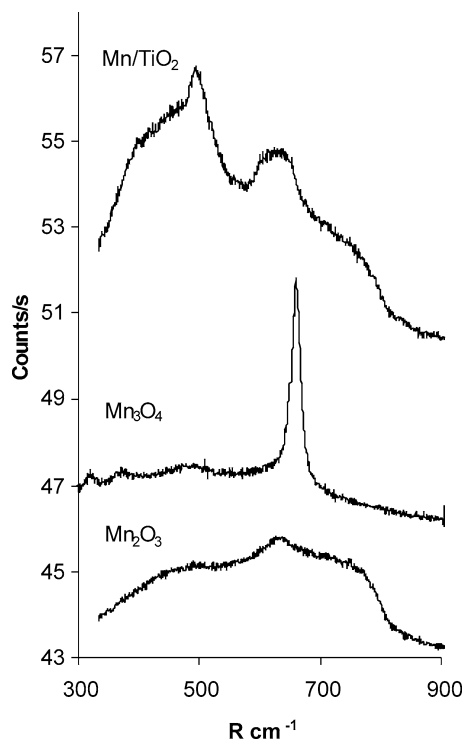


Fig. 2. Raman spectra of 20 wt% Mn/TiO₂, Mn₃O₄, and Mn₂O₃ collected at ambient conditions at 2 mW with an Ar laser.

be detected for Mn in deconvoluted XPS spectra (MnO₂ and Mn₂O₃), indicating the presence of these mixed metal oxide phases over the TiO₂ supports. It is well known that Mn₂O₃ is more amorphous than MnO₂ [30,31], indicating the difficulty of its detection by XRD. The Raman spectra presented in Fig. 2 could not help identify the different phases of manganese oxides, as the spectrum for Mn/TiO₂ is dominated by the titania peaks discussed above. However, the Raman spectra for the catalyst Mn/TiO₂ as shown in Fig. 2 show the broadening of the peaks throughout the scanned region, 325–900 cm⁻¹. Kapteijn et al. [32] have reported the possible presence of manganese oxide phases in their Raman spectra in the region of 635–650 cm⁻¹, indicating that the Raman spectra for Mn/TiO₂ may have the presence of Mn-oxide phases. Moreover, Bernard et al. [33] have reported

that, although part of MnO_2 transforms into haussmanite (Mn_3O_4 , 651 cm^{-1}) due to the pressure used during the pellets formation of MnO_2 powder, the spectrum of MnO_2 shows three main peaks in its Raman spectra, viz. 650, 576, and 523 cm^{-1} . Also, the Raman spectra for Mn_2O_3 is also reported [33] to show peaks at 581, 509 (broad), and 630 cm^{-1} (shoulder). Hence, taking the above points into account and our own quite complex and broad Raman spectra for Mn/TiO_2 (Fig. 2), we may conclude that the presence of various phases for Mn oxide (viz. MnO_2 , Mn_2O_3 , and Mn_3O_4) are likely to be present.

Fig. 1 also shows the presence of Co_3O_4 (JCPDS File No. 43-1003) and NiO (JCPDS File No. 44-1159) as weak crystalline phases for cobalt and nickel oxides supported on TiO_2 , respectively. No XRD phases were observed for TiO_2 -supported Cu- and Cr-oxide catalysts. Additionally, crystalline phases could not be observed in the XRD spectra of V/TiO_2 and Fe/TiO_2 . This could also be attributed to their amorphous nature. This was most apparent in the case of V/TiO_2 , which did not produce a single peak in the XRD spectrum (not shown). The surprising disappearance of all XRD peaks, including titania, in this catalyst indicates that the support could be completely covered with vanadia due to its very high loading, 20 wt%, further indicating the highly amorphous nature of vanadia. It is reported in the literature [34,35] that vanadia is normally well dispersed on titania and silica supports. As a result, no corresponding XRD peak could be detected at 27.2 wt% vanadium loading.

3.3. X-ray photoelectron spectroscopy

The surface atomic concentrations for oxygen, titanium, and transition metals and the atomic ratios for V/Ti, Cr/Ti, and Ni/Ti are presented in Table 2. The atomic concentrations were based upon the binding energies observed for O 1s, Mn 2p, Cr 2p, Ni 2p, and V 2p in the titania-supported transition metal oxide catalysts. All the values are referenced to the Ti $2p_{3/2}$ BE value of 458.5 eV. This peak was chosen for its clarity, intensity, lack of contaminant interference, and the absence of other oxidation states. It is remarkable to note the very high Mn/Ti atomic ratio of 5.9 that was observed for 20 wt% Mn/TiO_2 when calcined at 673 K, indi-

Table 2
Atomic surface concentrations of the catalysts as determined by XPS

Catalyst composition ^a	Calcination temperature (K)	Atomic concentrations (%) ^b			
		Oxygen	Titanium	TM	TM/Ti
V/TiO_2	673	58.1	14.0	5.5	0.4
Cr/TiO_2	673	53.5	5.4	9.2	1.7
Mn/TiO_2	673	52.3	3.5	20.8	5.9
Mn/TiO_2	873	51.6	13.2	6.6	0.5
Ni/TiO_2	673	53.2	12.6	1.4	0.1

^a 20 wt% metal loading.

^b Mg-K α radiation at 300 W, 89.45- and 35.75-eV pass energies; the remaining mass for each catalyst consisted of carbon.

ating a substantial amount of Mn on the surface. However, when the same catalyst was calcined at the higher temperature of 873 K, the Mn/Ti ratio severely decreased to 0.5. This may be due to the diffusion of the metal oxide, MnO_x , into the TiO_2 matrix and/or due to its sintering leading to the decreased catalytic activity as discussed in the following section. Additionally, the surface concentration of other transition metals was poor. The lowest ratio of 0.1 was observed for Ni. For Ni/TiO_2 , NiO seems to be mostly buried under titania and may not be available on the surface for the catalytic reaction.

The XPS spectra for O 1s is given in Fig. 3 and shows that the deconvoluted O 1s spectra gave two distinct peaks. The lower BE peak is due to oxygen from TiO_2 , whereas the higher BE peak is due to the respective transition metal oxides. From Fig. 3 it is clear that the surface oxygen concentration in Mn/TiO_2 is quite high as compared to that for Cr/TiO_2 and Ni/TiO_2 catalysts. The Ti $2p_{3/2}$ (Fig. 4) spectra

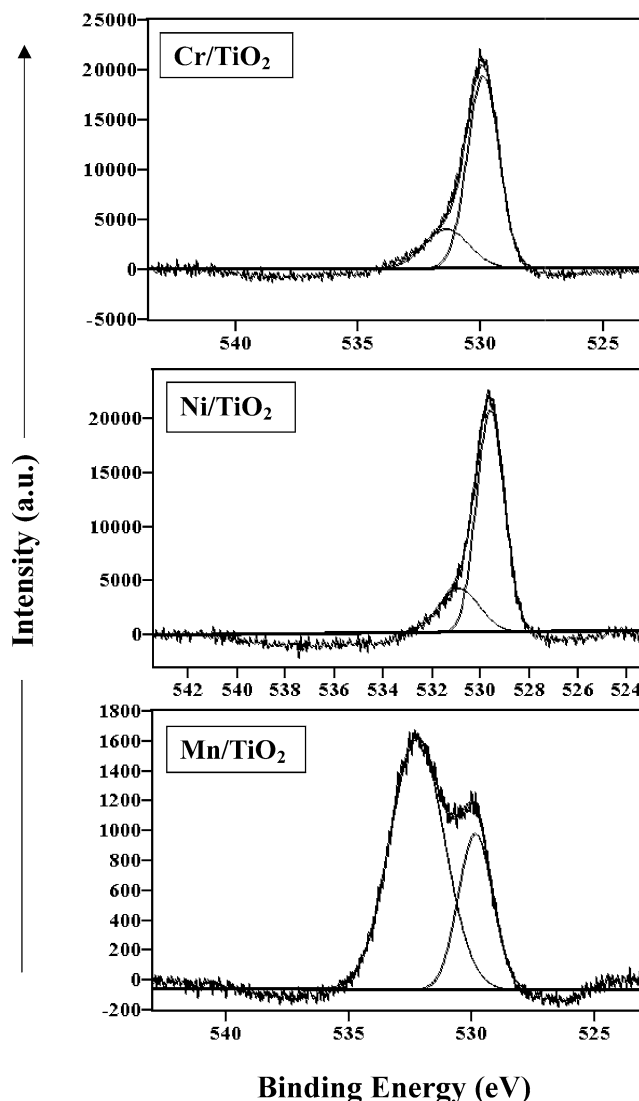


Fig. 3. O 1s XPS spectra of Cr/TiO_2 , Ni/TiO_2 , and Mn/TiO_2 (20 wt% metal loading).

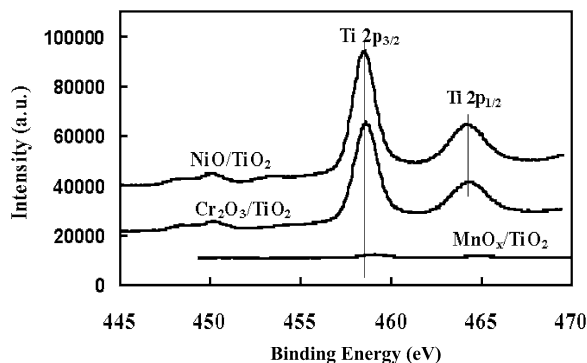


Fig. 4. Ti 2*p* XPS spectra of Ni/TiO₂, Cr/TiO₂, and Mn/TiO₂ (20 wt% metal loading).

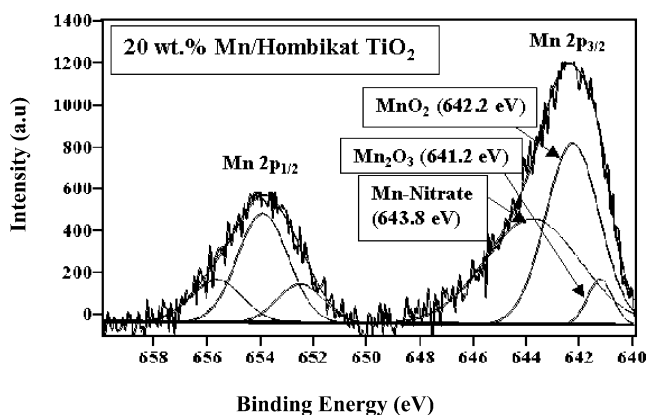


Fig. 5. Deconvoluted XPS results of Mn 2*p* for 20 wt% Mn/TiO₂.

comparing Ni, Cr, and Mn oxides supported on TiO₂ catalysts are shown in Fig. 4. It is evident from Fig. 4 that the concentration of Ti 2*p*_{3/2} and thus that of TiO₂ catalyst is significantly less compared to Cr/TiO₂ and Ni/TiO₂ catalysts. This is probably due to the higher surface coverage by Mn oxide and/or its higher dispersion on the TiO₂ support as reported earlier by Kapteijn et al. [32] for Mn/Al₂O₃ catalysts. This clearly indicates that the concentration of Mn on the surface of Mn/TiO₂ relative to the support is significantly higher than the other metal oxides. The Mn 2*p* spectra for 20 wt% Mn/TiO₂ were deconvoluted to obtain detailed information on the presence of possible metal oxide phases and their relative intensities. The spectrum shows (Fig. 5) the presence of three peaks corresponding to Mn₂O₃ (641.2 ± 0.2 eV), MnO₂ (642.2 ± 0.4 eV) [32], and Mn-nitrate at 644.2 ± 0.4 eV. The Mn-nitrate peak is expected, as the catalysts were calcined at a relatively low temperature of 673 K. It should be noted that no reference in the literature was found to verify our claim that the peak near 644 eV could be due to Mn-nitrate. Therefore, in order to confirm the presence of partially undecomposed nitrate species in the catalysts calcined at lower temperatures, an uncalcined catalyst was analyzed using XPS. The prominent peak at 644.5 eV belonging to Mn-nitrate was visibly seen, confirming our claim of the presence of nitrate species for our catalysts calcined at lower temperatures. Moreover, this

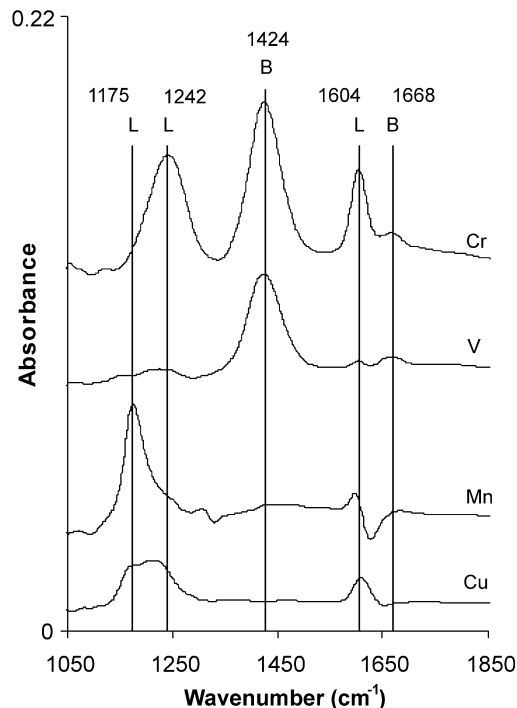


Fig. 6. FT-IR spectra of adsorbed species after contact with ammonia for various transition metal oxides supported on TiO₂ after outgassing at 373 K (B, Brönsted acid site; L, Lewis acid site).

peak disappeared for the catalysts calcined at 873 K. The confirmation of MnO₂ and Mn₂O₃ from our deconvoluted XPS spectra may be used as evidence to conclude that supported metal oxides active in low-temperature SCR of NO_x are present in at least two different oxidation states, possibly suggesting a redox mechanism for the low-temperature SCR reaction.

3.4. Acidity characterization of the catalysts

3.4.1. NH₃ FT-IR

The spectra of ammonia adsorbed on V, Cr, Mn, and Cu oxides supported on TiO₂ after outgassing at 373 K are compiled in Fig. 6. All the spectra were normalized and recorded under identical operating conditions. It is reported in the literature that anatase TiO₂ adsorbs ammonia in coordinated form over Lewis acid sites [36,37]. This indicates that anatase TiO₂ is purely Lewis acidic and any evolution of Brönsted acid sites should be related to the metal oxides deposited on TiO₂ supports. Fig. 6 shows the presence of four prominent bands near 1175 cm⁻¹ (Lewis acid sites), 1242 cm⁻¹ (Lewis acid sites), 1424 cm⁻¹ (Brönsted acid sites), and 1604 cm⁻¹ (Lewis acid sites). Based upon the number and size of the peaks observed over Cr/TiO₂, this catalyst clearly possesses the greatest amount of surface acidity. V/TiO₂ only possessed significant amounts of Brönsted acidity, while both Mn/TiO₂ and Cu/TiO₂ only had significant amounts of Lewis acid sites. Kapteijn et al. [38] also reported in the case of alumina-supported manganese oxide catalysts that the addition of Mn to alumina does not

induce any Brønsted acidity. The mix of Lewis and Brønsted acid sites along with recording the spectra under actual reaction conditions served to help identify the surface characteristics necessary for operation at low temperatures. As it will be shown in the discussion of catalytic activity, Brønsted acid sites do not appear to be necessary to carry out the reaction. An exhaustive study describing the adsorption–desorption characteristics of the gases, viz. NH_3 , NO , or O_2 or the mixture of the two or more gases, especially on Mn/TiO_2 catalyst by in situ FT-IR has been thoroughly investigated in the subsequent paper [39].

3.4.2. NH_3 -TPD

The amount and strength of the acid sites in the samples were probed by NH_3 -TPD. Fig. 7 shows the ammonia desorption patterns for various transition metal oxides supported on TiO_2 . The total acidity of various catalysts is summarized in Table 1. Except for V and Cu, the rest of the metal oxides supported on TiO_2 distinctly show the presence of broadly distributed strong acid sites that continue desorbing above 523 K. When TPD curves for Mn and V supported on TiO_2 are compared, the overall area of ammonia desorption curve for the latter catalyst is much smaller than that of the former one. It should be remembered that not a single XRD peak was detected for V/TiO_2 , most probably due to the amorphous nature of vanadium. This suggests that ammonia that could have been adsorbed on titania acid sites was absent in this catalyst resulting in an overall decrease in acidity and corresponding loss in catalytic activity. It is often reported in the literature [36,40] that ammonia adsorbed on Brønsted acid sites desorbs easier than Lewis-coordinated ammonia during temperature-programmed desorption. This

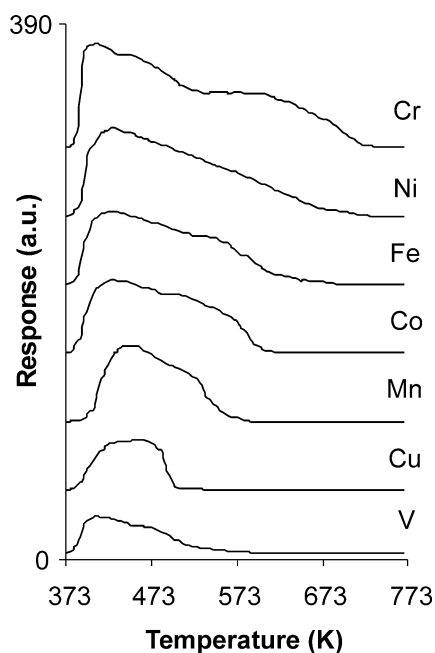


Fig. 7. NH_3 -TPD spectra of various transition metals TiO_2 (20 wt% metal loading).

was observed in our NH_3 FT-IR experiments as well (not shown).

3.5. Catalytic activity

3.5.1. Results at low GHSV (8000 h^{-1})

The performance of various catalysts for low-temperature SCR at reaction temperatures of 373 and 393 K operating under identical experimental conditions is presented in Fig. 8. The data show that catalysts with Cr, Mn, and Cu are highly active at low temperature, and quantitative NO conversion is achieved at 393 K with 100% N_2 selectivity for 20 wt% Mn/Hombikat TiO_2 catalyst. N_2O and NO_2 were not detected with our mass spectrometer. It should be noted here that a much higher NO concentration (2000 ppm) was used for this set of our experiments than that found in the flue gas of industrial power plants at the tail end. As we have demonstrated earlier [24,25] and as we show below (case of $50,000 \text{ h}^{-1}$) in this paper, the Mn-based catalysts are equally effective for space velocities and operating conditions found in industry. The other important factor could be the possible redox behavior of our catalysts, which was presented earlier with the XPS results. Very recently Yang and others [41,42] have also reported active catalysts, viz. Fe–Mn [41] and MnO_x – CeO_2 [42], for the low temperature (373–453 K) SCR of NO with NH_3 at relatively high space velocities of 15,000 and $42,000 \text{ h}^{-1}$, respectively, but using relatively lower concentrations of NO (1000 ppm) in the feed. V/TiO_2 , which is the catalyst of choice in commercial medium temperature De NO_x systems, was found to be ineffective in our study. The poor catalytic activity for the Ni-based catalyst suggests that it may be in its reduced form even under oxidizing conditions and/or is predisposed to monovalent oxidation behavior. Moreover, the surface concentration of nickel on TiO_2 (Table 2) is also very small ($\text{Ni}/\text{Ti} = 0.1$) compared to the other metals. This could also be the reason why this particular catalyst is not active in our system. It is believed that the high surface concentration of active metal oxides on the surface, the ability of the metal oxide to operate in the redox mode, and Lewis acidity are the main contributors to excellent performance at these conditions.

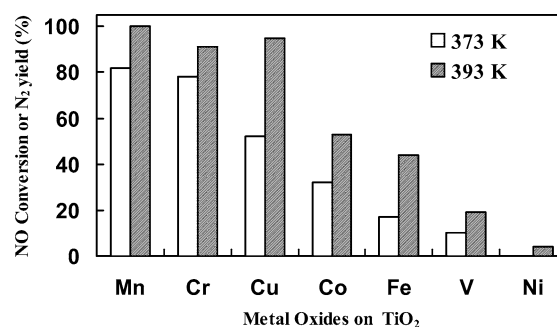


Fig. 8. Performance of 20 wt% transition metal/ TiO_2 catalysts at 373 and 393 K (GHSV = 8000 h^{-1} , $\text{NO} = \text{NH}_3 = 2000 \text{ ppm}$, 2.0 vol% O_2 , He balance).

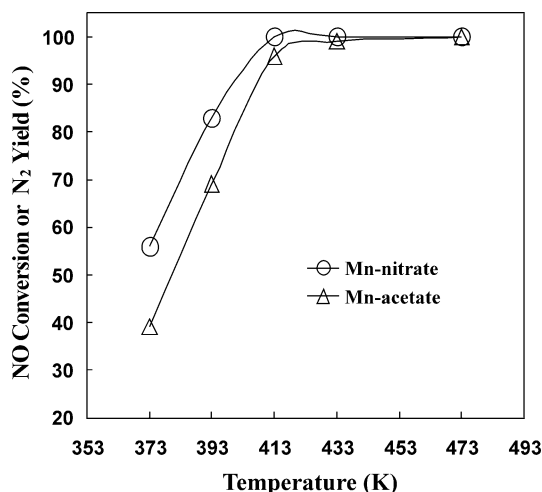


Fig. 9. Comparison of manganese precursors (5.0 wt% Mn) supported on TiO_2 at different temperatures (GHSV = 8000 h^{-1} , $\text{NO} = \text{NH}_3 = 2000 \text{ ppm}$, 2.0 vol% O_2 , He balance).

After finding $\text{MnO}_x/\text{TiO}_2$ to be the most active catalyst, the role of the Mn precursor was examined. As shown in Fig. 9, a catalyst prepared from Mn-nitrate gives better performance than one prepared from the acetate precursor under these conditions. The higher surface area of the catalyst prepared from the nitrate precursor and the formation of MnO_2 as the major and active phase could be the reasons. In contrast to our results, Kapteijn et al. [43] have reported that manganese acetate results in better dispersion of manganese oxide on alumina and higher catalytic activity than manganese nitrate at 373–453 K. That group concluded from H_2 TPR studies that acetate yields Mn_2O_3 while nitrate produces mainly MnO_2 . At the same time, the authors claimed that MnO_2 exhibits higher NO reduction activity than Mn_2O_3 per unit surface area. This explanation clearly indicates that MnO_2 should be more active than Mn_2O_3 in SCR reactions based upon our XPS results (Fig. 5). We could clearly observe the presence of MnO_2 in our catalysts along with better catalytic performance than the previously reported catalysts. It should be noted that higher loadings of Mn on the titania support gave better results, and this will be discussed below. Surprisingly, V/TiO_2 was found to be totally inactive for SCR reaction at low temperatures. In our study the actual surface area for the TiO_2 support decreased by about 5 times after vanadium deposition. Other metal oxides do not lead to such a drastic decrease in surface area (Table 1).

Mn loadings ranging from 5 to 25 wt% were studied at reaction temperatures of 373 and 393 K. The results are presented in Fig. 10. NO conversion increases with an increase in metal loading, and an optimum loading is observed near 20 wt% Mn. At 393 K quantitative NO conversion is achieved at 17.5 wt% Mn loading. The selectivity for N_2 was always 100% irrespective of catalytic activity. Catalysts having lower Mn loadings, along with those having higher loadings but calcined at higher temperatures, do not per-

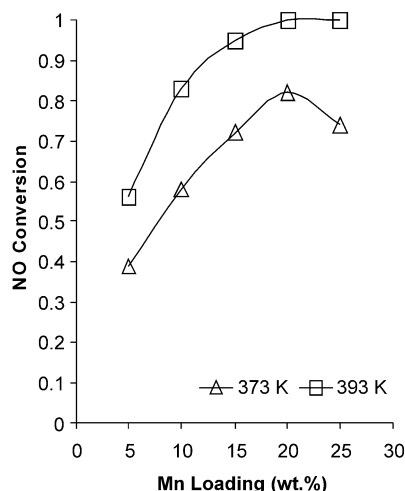


Fig. 10. Catalytic performance of Mn (nitrate)/ TiO_2 as a function of metal loading at 373 and 393 K (GHSV = 8000 h^{-1} , $\text{NO} = \text{NH}_3 = 2000 \text{ ppm}$, 2.0 vol% O_2 , He balance).

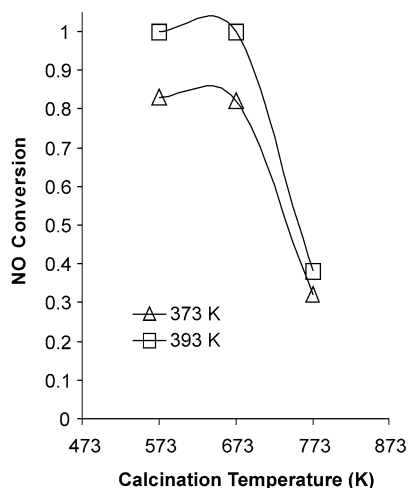


Fig. 11. Catalytic performance of Mn (nitrate)/ TiO_2 as a function of calcination temperature at 373 and 393 K (GHSV = 8000 h^{-1} , $\text{NO} = \text{NH}_3 = 2000 \text{ ppm}$, 2.0 vol% O_2 , He balance, 20 wt% Mn).

form well. Only catalysts with higher Mn loadings which are calcined at lower temperatures provide excellent catalytic performance (Fig. 11). H_2 TPR results for the catalysts are shown in Fig. 12. The results show that higher reduction temperatures are needed for catalysts synthesized with lower Mn loadings or calcined at higher temperatures. For these catalysts, there is likely to be a stronger metal–support interaction especially when the catalysts are calcined at higher temperatures (> 673 K), thereby making it more difficult to carry out the reduction. A similar trend was observed by Richter et al. [44]. Increasing Mn loading decreases the temperature required for reduction of MnO_x , provided that the catalysts are calcined at or below 673 K. In summary, the catalysts with higher metal loadings and lower calcination temperature provided the best catalytic performance, and the lower reduction temperatures observed in those cases

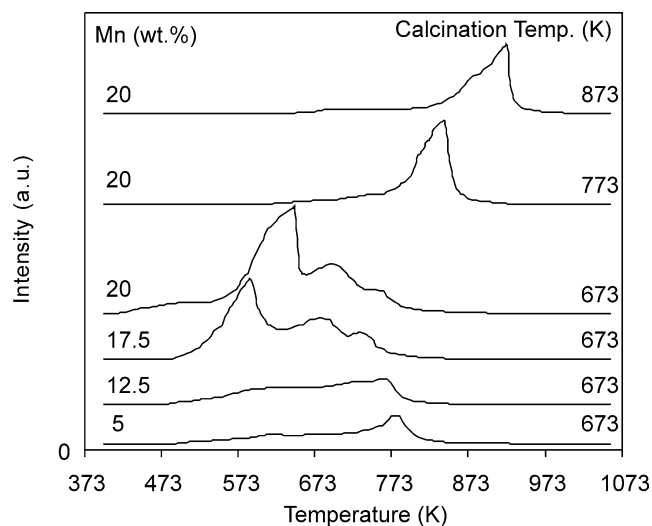


Fig. 12. H_2 TPR of MnO_x/TiO_2 catalysts (with different Mn loadings and prepared using Mn-nitrate precursor).

suggest the presence of MnO_2 (major) and Mn_2O_3 (minor) phases [10,43].

It is reported [45] that crystallites of V_2O_5 are formed at the expense of polymeric vanadyl species if the vanadia loading exceeds a theoretical monolayer. Crystalline V_2O_5 species are detrimental to both activity and N_2 selectivity. Those in situ Raman spectroscopic studies revealed that NH_3 is chemisorbed on Ti^{4+} centers associated with the support and that the coordination of NH_3 takes place only with the isolated monomeric vanadyl species. We confirmed from our XRD studies that high loading vanadia/titania catalysts do not yield any XRD peaks, indicating that titania is completely covered with homogeneously dispersed V_2O_5 species. Hence, there is no chance for NH_3 to be adsorbed on crucial Ti^{4+} sites of the support, and that could lead to its subsequent dissociation on monomeric vanadyl species. The NH_3 -TPD results also indicated that the V/TiO_2 catalyst adsorbs very small quantities of NH_3 , further indicating its relatively low acidity (Fig. 7). It can be concluded that the higher amount of Brönsted acidity, possible coverage of the titania support by amorphous V oxide, very low overall acidity, and the low surface area of the actual catalyst relative to the support could be the main reasons for its dismal catalytic performance at the lower temperatures. In addition to this, the catalyst may not have the required activation energy for this reaction at these temperatures. In contrast with the reported literature for medium-temperature SCR operations [46–50] where it is reported that Brönsted acidity is of utmost importance to obtain better catalytic activity, we have shown here that Lewis acidity is important in our system and that in our best catalyst, MnO_x/TiO_2 , the most active phase found from XRD and XPS observations was MnO_2 .

3.5.2. Results at higher GHSV of $50,000 h^{-1}$

Since SCR catalysts used in power plants will typically be used at GHSV values above $30,000 h^{-1}$, all of the ca-

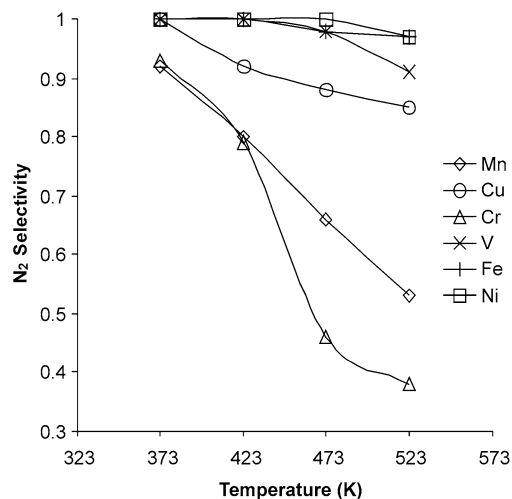
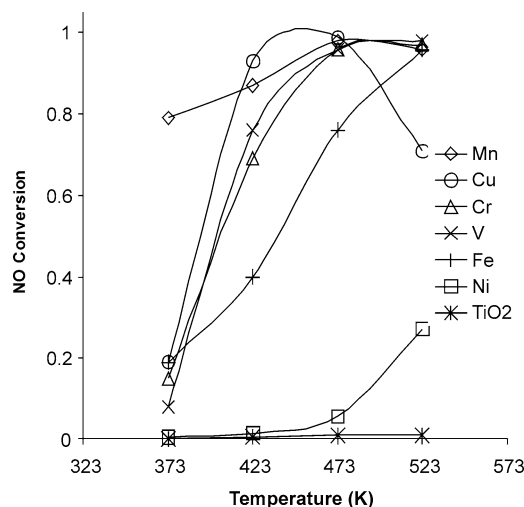


Fig. 13. Catalytic performance of transition metals supported on TiO_2 as a function of temperature (20 wt% metal loading, GHSV = $50,000 h^{-1}$, $NO = NH_3 = 400 ppm$, 2.0 vol% O_2 , He balance).

lysts previously discussed were tested at $50,000 h^{-1}$. The NO conversion and N_2 selectivity results are presented in Fig. 13. While it is expected that the catalytic activity would not be as high as that reported at $8000 h^{-1}$, MnO_x/TiO_2 provides respectable catalytic activity relative to the other transition metals tested at temperatures below 423 K. Cu/TiO_2 also provides high catalytic activity under these conditions and peaks in activity from 423 to 473 K. Mn is clearly most useful at temperatures below 423 K, as its N_2 selectivity quickly declines below 90% as the temperature increases. It appears that Cu/TiO_2 outperforms Mn/TiO_2 at higher space velocities when both the activity and the selectivity data are considered; however, SCR units in power plants must have N_2 selectivities above 95% to avoid releasing significant amounts of N_2O into the atmosphere. Additionally, industrial SCR units will be exposed to significant amounts of water from combustion. Consequently, the catalytic performance of all the supported transition metal oxides tested

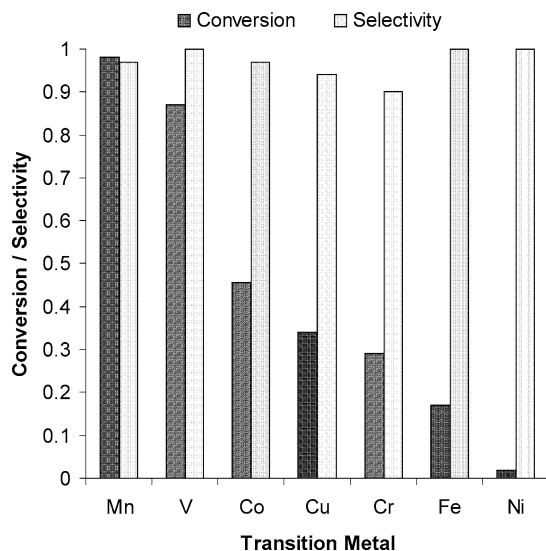


Fig. 14. Catalytic performance of transition metals supported on TiO₂ at 448 K (20 wt% metal loading, GHSV = 50,000 h⁻¹, NO = NH₃ = 400 ppm, 2.0 vol% O₂, 11 vol% H₂O, He balance).

in the presence of 11 vol% water is presented in Fig. 14 at 448 K and 400 ppm NO in the feed. As it can clearly be seen, Mn/TiO₂ provides the best overall performance when water is present. The presence of water drastically suppresses the formation of N₂O, allowing the use of Mn/TiO₂ at slightly higher temperatures. This suggests that water preferentially adsorbs on the active sites responsible for the N₂O formation, and this phenomenon is beneficial for the application of Mn/TiO₂ catalysts in power plants. Under these conditions, the catalytic activity of the transition metal oxides decreases in the following order: Mn > V ≫ Co > Cu > Cr > Fe ≫ Ni.

4. Conclusions

Most of the catalysts studied, which included Mn, Fe, Co, Ni, and Cu supported on titania, possessed mainly Lewis acidity and had relatively weak Brønsted acid sites. Only Cr/TiO₂ and V/TiO₂ possessed a significantly high amount of Brønsted acidity, and that was coupled with a substantial amount of Lewis acidity for Cr/TiO₂. Comparing the low-temperature (373 K) SCR activity of our catalysts, it was concluded that catalysts having Lewis acidity are active and that Brønsted acidity may not be contributing to catalytic performance, as reported earlier by Busca and co-workers [36]. The deposition of active metal oxide(s), in addition to the catalyst preparation method, is paramount to excellent catalytic activity at temperatures as low as 393 K. In the case of V/TiO₂, it was concluded that high levels of Brønsted acidity, complete coverage of titania by vanadium oxide, inability of the catalyst to activate at low temperatures, very low overall acidity, and the low surface area of the actual catalyst as compared to the support were the main reasons for its dismal catalytic performance in low-temperature

SCR of NO with NH₃. The H₂ TPR study over MnO_x/TiO₂ suggested that a higher reduction temperature was required when either the Mn loading was low (≤ 12.5 wt%) or the catalysts were calcined at higher temperatures (≥ 773 K). In MnO_x/TiO₂ catalysts, XPS and XRD studies showed the presence of MnO₂ (major) and Mn₂O₃ (minor) phases. Since MnO₂ is present in higher concentrations, it is suggested to be the most active phase for low-temperature SCR of NO with NH₃. Catalytic experiments performed at 50,000 h⁻¹ with 11 vol% water demonstrated that MnO_x/TiO₂ was the most promising catalyst for low temperature SCR applications. Evidently, the presence of water increased N₂ selectivity by preferentially adsorbing on those active sites responsible for the formation of N₂O.

Acknowledgments

The authors are grateful to the Ohio Coal Development Office (OCDO), Columbus, Ohio, USA, for financial support and for allowing us to publish our findings. The authors thank Dr. Ettireddy Padmanabha Reddy for thoughtful discussions.

References

- [1] H. Bosch, F. Janssen, *Catal. Today* 2 (1988) 369.
- [2] J.G. Henry, G.W. Heinke, *Environmental Science and Engineering*, Prentice-Hall, Englewood Cliffs, NJ, 1989.
- [3] F. Luck, J. Roiron, *Catal. Today* 4 (1989) 205.
- [4] F. Janssen, F. van den Kerkhof, H. Bosch, J.R.H. Ross, *J. Phys. Chem.* 91 (1987) 5921.
- [5] J.W. Byrne, J.M. Chen, B.K. Spononello, *Catal. Today* 13 (1992) 33.
- [6] G. Ramis, G. Busca, F. Bregani, *Catal. Lett.* 139 (1993) 353.
- [7] S.C. Wood, *Chem. Eng. Progr.* 90 (1994) 32.
- [8] L.J. Alemany, F. Berti, G. Busca, G. Ramis, D. Robba, G.P. Toledo, M. Trombetta, *Appl. Catal. B* 248 (1996) 299.
- [9] J.A. Dumesic, N.-Y. Topsoe, H. Topsoe, T. Slabick, *J. Catal.* 163 (1996) 409.
- [10] L. Singoredjo, R. Korver, F. Kapteijn, J.A. Moulijn, *Appl. Catal. B* 1 (1992) 297.
- [11] W.S. Kijlstra, D.S. Brands, H.I. Smit, E.K. Poels, A. Bliet, *J. Catal.* 171 (1997) 219.
- [12] W.S. Kijlstra, E.K. Poels, A. Bliet, B.M. Weckhuysen, R.A. Schoonheydt, *J. Phys. Chem. B* 101 (1997) 309.
- [13] G. Centi, S. Perathoner, D. Biglino, E. Giamello, *J. Catal.* 151 (1995) 75.
- [14] G. Ramis, L. Yi, G. Busca, M. Turco, E. Kotur, R.J. Willey, *J. Catal.* 157 (1995) 523.
- [15] A. Kato, S. Matsuda, F. Nakajima, M. Imanari, Y. Watanabe, *J. Phys. Chem.* 85 (1981) 1710.
- [16] S. Kasaoka, E. Sasaoka, H. Iwasaki, *Bull. Chem. Soc. Jpn.* 62 (1989) 1226.
- [17] J. Pasel, P. Käbner, B. Montanari, M. Gazzano, A. Vaccari, W. Makowski, T. Lojewski, R. Dziembaj, H. Papp, *Appl. Catal. B* 18 (1998) 199.
- [18] M. Yoshikawa, A. Yasutake, L. Mochida, *Appl. Catal. A* 173 (1998) 239.
- [19] Z. Zhu, Z. Liu, S. Liu, H. Niu, *Appl. Catal. B* 23 (1999) L229.
- [20] Z. Zhu, Z. Liu, H. Niu, S. Liu, *J. Catal.* 187 (1999) 245.
- [21] E. Richter, *Catal. Today* 7 (1990) 93.

- [22] C.J.G. Van der Grift, A.F. Woldhuis, O.L. Maaskant, *Catal. Today* 27 (1996) 23.
- [23] V. Visciglio, G. Blanchard, R. Surantyn, *Catal. Lett.* 40 (1996) 39.
- [24] P.G. Smirniotis, D.A. Peña, B.S. Uphade, US patent applied, filed 2000.
- [25] P.G. Smirniotis, D.A. Peña, B.S. Uphade, *Angew. Chem. Int. Ed. Engl.* 40 (2001) 2479.
- [26] N.V. Economidis, D.A. Peña, P.G. Smirniotis, *Appl. Catal. B* 23 (1999) 123.
- [27] I. Barin, *Thermochemical Data of Pure Substances*, Chemie, Berlin, 1989.
- [28] J.L. Alemany, L. Lietti, N. Ferlazzo, P. Forzatti, G. Busca, G. Ramis, E. Giamello, F. Bregani, *J. Catal.* 155 (1995) 117.
- [29] G. Busca, G. Ramis, J.M.G. Amores, V.S. Escibano, P. Piaggio, *J. Chem. Soc., Faraday Trans.* 90 (1994) 3181.
- [30] E.R. Stobbe, B.A. de Boer, J.W. Geus, *Catal. Today* 47 (1999) 161.
- [31] J. Datka, A.M. Turek, J.M. Jehng, I.E. Wachs, *J. Catal.* 135 (1992) 186.
- [32] F. Kapteijn, A.D. van Langeveld, J.A. Moulijn, A. Andreini, M.A. Vuurman, A.M. Turek, J.-M. Jehng, I.E. Wachs, *J. Catal.* 150 (1994) 94.
- [33] M.-C. Bernard, A.H.-L. Goff, B.V. Thi, S.C. de Torresi, *J. Electrochem. Soc.* 140 (1993) 3065.
- [34] M.A. Reiche, Ortelli, A. Baiker, *Appl. Catal. B* 23 (1999) 187.
- [35] H. Miyata, K. Fujii, T. Ono, *J. Chem. Soc., Faraday Trans. I* 84 (1988) 3121.
- [36] J.M.G. Amores, V.S. Escibano, G. Ramis, G. Busca, *Appl. Catal. B* 13 (1997) 45.
- [37] G. Busca, L. Lietti, G. Ramis, F. Berti, *Appl. Catal. B* 18 (1998) 1.
- [38] F. Kapteijn, L. Singoredjo, M. van Driel, A. Andreini, J.A. Moulijn, G. Busca, G. Ramis, *J. Catal.* 150 (1994) 105.
- [39] D.A. Peña, E.P. Reddy, B.S. Uphade, P.G. Smirniotis, in preparation.
- [40] L. Lietti, G. Ramis, F. Berti, G. Toledo, D. Robba, G. Busca, P. Forzatti, *Catal. Today* 42 (1998) 101.
- [41] R.Q. Long, R.T. Yang, R. Chang, *Chem. Commun.* (2002) 452.
- [42] G. Qi, R.T. Yang, *Chem. Commun.* (2003) 848.
- [43] F. Kapteijn, L. Singoredjo, A. Andreini, J.A. Moulijn, *Appl. Catal. A* 3 (1994) 173.
- [44] M. Richter, A. Trunschke, U. Bentrup, K.-W. Brzezinka, E. Schreier, M. Schneider, M.-M. Pohl, R. Fricke, *J. Catal.* 206 (2002) 98.
- [45] G.T. Went, L.-J. Leu, R.R. Rosin, A.T. Bell, *J. Catal.* 134 (1992) 492.
- [46] N.-Y. Topsøe, *J. Catal.* 128 (1991) 499.
- [47] N.-Y. Topsøe, *Science* 265 (1994) 1217.
- [48] N.-Y. Topsøe, H. Topsøe, J.A. Dumesic, *J. Catal.* 151 (1995) 226.
- [49] H. Schneider, S. Tschudin, M. Schneider, A. Wokaun, A. Baiker, *J. Catal.* 147 (1994) 5.
- [50] N.-Y. Topsøe, J.A. Dumesic, H. Topsøe, *J. Catal.* 151 (1995) 241.